Biochemistry (Moscow), Vol. 62, No. 3, 1997, pp. 251-263. Translated from Biokhimiya, Vol. 62, No. 3, pp. 296-309.

Composition and Structural and Functional Properties of Discoidal and Spherical Phospholipid–ApoE3 Complexes

M. De Pauw,[1] B. Vanloo,[1] A. D. Dergunov,[2,3] A.-M. Devreese,[1] J. Baert,[4] R. Brasseur,[5] and M. Rosseneu[1]

Submitted June 25, 1996; revision submitted November 20, 1996.

To model the common structural unit in the system of reverse cholesterol transport, we studied the composition, structure, and physicochemical properties of complexes generated between dipalmitoylphosphatidylcholine (DPPC) or palmitoyllinoleoylphosphatidylcholine (PLPC) and apoE3 in the absence and in the presence of cholesterol (Chol); the data were compared with similar experiments using apoA-I, the major protein of high-density lipoproteins. The conformation and organization of lipid-binding domains of apoE3 within the complexes were calculated by computer modeling. The transition temperatures of DPPC within discoidal complexes with mean diameters of 116 Å (GGE) or 148 Å (EM) were higher for complexes versus liposomes both in the absence and in the presence of Chol. Association of apoE3 with DPPC resulted in a more structured state of the apolipoprotein molecule versus the soluble apolipoprotein; this state was characterized by parallel orientation of α-helixes of apoE3 and DPPC acyl chains. Substrate efficiency of the apoE3–PLPC–Chol complexes in the lecithin-cholesterol acyltransferase (LCAT) reaction expressed as V_{max}/K_m was 0.5 nmole cholesteryl esters/h per 1 μM. The transformation of discoidal apoE3–DPPC–Chol complexes into spherical particles was induced by LCAT and accumulation of cholesteryl esters was ~62% of the total cholesterol. Parallel orientation of phospholipid acyl chains with helical segments disappeared in these particles. Discoidal apoE3–DPPC complexes incorporated unesterified cholesterol released from Chol-loaded J774 macrophages. The data support the concept that association of apoE3 and apoA-I with phospholipids is qualitatively similar due to similar orientation of helical repeats in the C-terminal domains of apoE3 and apoA-I.

KEY WORDS: apolipoprotein E, cholesterol efflux, lecithin-cholesterol acyltransferase, lipid–protein interaction.

Apolipoprotein E plays an important role in cholesterol metabolism because it is a high-affinity ligand for the cellular apoB,E-receptor. This apolipoprotein is thereby involved in the catabolism of several lipoprotein classes, including very low-density lipoproteins (VLDL)[6], chylomicron remnants, and so-called "pathological" lipoproteins [1, 2]. The primary structure of apoE has been determined both by protein [3] and by cDNA sequencing [4, 5]. Cysteine-arginine interchanges at residues 112 and 158 result in the existence of three major apolipoprotein isoforms—apoE4, apoE3, and apoE2—and have a major impact on the structure and function of apoE. ApoE consists of three major functional domains: the N-terminal domain spanning residues 1-191, an intermediate domain residues 192-215, and the C-terminal domain from residue 216 to 299. The crystal structure of the N-terminal domain of apoE shows that it consists of a four-helix bundle oriented in antiparallel fashion [6]. This region includes the receptor binding domain of apoE,

[1]Department of Biochemistry, University of Ghent, Belgium; fax: (3209) 225-34-89; E-mail: Maryvonne.Rosseneu@rug.ac.be
[2]Department of Biochemistry, Research Center for Preventive Medicine, Petroverigsky per. 10, Moscow, 101953 Russia; fax: (7-095) 928-50-63; E-mail: eqa@glas.apc.org
[3]To whom correspondence should be addressed.
[4]Interdisciplinary Research Center, University of Leuven Campus Kortrijk, Belgium.
[5]Laboratoire Chimie des Macromolecules aux Interfaces, Free University Brussels, Belgium.
[6]Abbreviations: CETP) cholesteryl ester transfer protein; DMPC) dimyristoylphosphatidylcholine; DPPC) dipalmitoylphosphatidylcholine; EM) electron microscopy; FCS) fetal calf serum; GdnHCl) guanidine hydrochloride; GGE) gradient gel electrophoresis; LCAT) lecithin-cholesterol acyltransferase; LPDS) lipoprotein-deficient serum; PLPC) palmitoyllinoleoylphosphatidylcholine; POPC) palmitoyloleoylphosphatidylcholine.

0006-2979/97/6203-0251$18.00 © 1997 МАИК Наука/Interperiodica Publishing

residues 140-160, which is highly helical and enriched in positively charged arginine residues.

Discoidal phospholipid–cholesterol–apolipoprotein complexes containing apoA-I, apoA-IV, and apoE represent nascent high-density lipoproteins (HDL) with apoA-I as the major protein constituent. They can be generated during lipolysis of triglyceride-rich VLDL or chylomicrons [7] and are also synthesized by the liver [8, 9]. The discoidal particles can accept Chol from the cell membrane with subsequent conversion into spherical mature HDL under the action of LCAT [7]; these steps represent initial events in the "reverse" Chol transport from peripheral tissues. It has been proposed that discoidal complexes containing apoE can act as efficient cholesterol acceptors when apoA-I is either absent or deficient in human plasma [10].

Macrophages loaded with cholesteryl esters or foam cells have been identified in early atherosclerotic lesions [11] and can be generated *in vitro* by incubation of macrophages with chemically modified LDL [12]. HDL, discoidal phospholipid–apolipoprotein complexes as well as isolated apolipoproteins A-I, A-II, C-III, and E were reported to remove cholesterol from loaded peritoneal macrophages [13]. It can be suggested that different acceptor and substrate properties of apoA-I- and apoE-containing particles in Chol efflux and in LCAT-catalyzed formation of cholesteryl esters may determine the overall efficiency of reverse Chol transport.

The aim of this study was to investigate the structural peculiarities of model discoidal complexes of "parent" apoE3 isoform with phospholipid and Chol and to compare them with analogous parameters of the complexes with apoA-I in an attempt to determine the factors controlling the different functional activities of the complexes and native HDL particles with different apolipoproteins. We studied composition, structural properties, and stability of apoE3-containing complexes and demonstrated LCAT-induced conversion of the discoidal apoE3–DPPC–Chol complexes into spherical particles in the presence of LDL particles as exogenous Chol donor. Kinetic parameters of LCAT-catalyzed formation of cholesteryl esters with the apoE3–PLPC–Chol complexes were measured also. We demonstrated high ability of the discoidal apoE3–DPPC complexes to induce cholesterol efflux from Chol-loaded macrophages with subsequent cholesterol esterification by LCAT when the enzyme was added to the incubation medium. The common similarity of structural organization of apoE and apoA-I within discoidal and spherical complexes and some quantitative differences in the interaction of apolipoprotein helical segments with phospholipid–Chol phase within complexes with different apolipoproteins is suggested; in particular, the content and dynamics of cholesterol molecules in the lipid region adjacent to apolipoprotein molecule ("boundary lipid") could differ.

MATERIALS AND METHODS

Computer Modeling of Helical Repeats of ApoE3. The helical repeats in apoE3 were identified using a hydrophobicity auto correlation matrix as previously reported [14]. We assume that the minimal structural and functional motif in the apoE sequence consists of pairs of α-helixes each of 17 residues separated by a 4-5-residue peptide. The most stable conformations, corresponding to the lowest energy levels, were calculated for the entire 39-residue segments (17-residue helix–4-5-residue peptide–17-residue helix). This was carried out through a systematic calculation of the torsional angles φ and ψ for the residues of the linker peptide using the stereo alphabet procedure [15]. The conformation with the lowest energy level was subsequently derived using a simplex minimization procedure [16]. For each pair of helixes separated by a 4-5-residue peptide, the lowest energy structure was calculated as the sum of London–Van der Waals energy, Coulomb's electrostatic energy, and potential energy of rotation of the torsional angles. Calculations were performed on an Olivetti PC486 microcomputer (Olivetti, Italy) equipped with an Intel 80486 processor (Intel, USA), using PC-PROT (Protein Analysis Program) and PC-TAMMO (Theoretical Analysis of Molecular Membrane Organization) programs.

Isolation and Purification of ApoE3. ApoE was purified from the VLDL fraction recovered after plasmapheresis of a patient with familial hypercholesterolemia. The apoE phenotype (E3/3) was determined by isoelectric focusing followed by immunoblotting [17]. VLDL were isolated by ultracentrifugation at a density of 1.03 g/cm^3 and delipidated with acetone–ethanol (1:1 v/v), followed by hexane–isopropanol (3:2 v/v), and finally with hexane. After delipidation, apoVLDL fraction was dried under N_2 and stored at –20°C. VLDL apolipoproteins were separated by gel filtration on a Superdex 200PG (Pharmacia, Sweden) column equilibrated with 10 mM Tris-HCl buffer (pH 8.0) with 0.15 M NaCl, 0.2 g/liter NaN_3, and 7 M urea. The purity of apoE-containing fractions was checked by sodium dodecyl sulfate polyacrylamide gel electrophoresis (SDS-PAGE) (8-25% SDS gel; Pharmacia LKB PhastSystem, Sweden). The isolated apolipoprotein was dialyzed against 5 mM NH_4HCO_3, lyophilized, and dissolved in 10 mM Tris-HCl buffer (pH 8.0) with 0.15 M NaCl, 1 mM NaN_3, 0.1 g/liter EDTA, and 0.3 M GdnHCl.

Preparation of Phospholipid–Apolipoprotein Complexes. Complexes of apoE with dipalmitoylphosphatidylcholine (DPPC, Sigma, USA) and palmitoyllinoleoylphos-

phatidylcholine (PLPC, Sigma) at phospholipid/protein ratio of 3:1 (w/w) and the corresponding complexes with cholesterol at phospholipid/cholesterol/protein ratio of 3:0.15:1 (w/w) were prepared using cholate dialysis procedure [18]. The mixture was incubated at 43°C for the complexes with DPPC and at 4°C for the complexes with PLPC for 16 h.

Complex Isolation and Characterization. All experiments were carried out on complexes isolated in a chromatography system (Waters, USA) by gel filtration on a Superose 6HR column (Pharmacia) eluted with 5 mM Tris-HCl buffer (pH 8.0) with 0.15 M NaCl and 0.2 g/liter NaN_3. Complexes were detected by optical density at 280 nm and by tryptophane emission at 330 nm. The composition and size of the complexes were determined for the fraction with maximal absorbance in the elution profile. Phospholipid and cholesterol in the isolated complexes were measured using commercially available kits (Biomérieux, France; Boehringer Mannheim, Germany) and apoE3 content by sandwich ELISA as described previously [19]. The size of the complexes was estimated by non-denaturing gel electrophoresis in a 8-25% polyacrylamide gradient gel (Pharmacia LKB PhastSystem). The gels were scanned with a laser densitometer (Pharmacia) and the Stokes radii were estimated in comparison with protein standards (Pharmacia). For electron microscopy (EM) examination, the complexes were negatively stained with potassium phosphotungstate (20 g/liter), pH 7.4, and 7 µl of the samples were applied to Formvar carbon-coated grids and examined in a Zeiss EM 10C transmission electron microscope (Zeiss, Germany) operating at 60 kV. The mean diameter and the size distribution of the complexes were calculated for 175 particles for each sample.

Fluorescence Measurements. Fluorescence measurements were performed on an Aminco SPF-500 spectrofluorimeter (Aminco, USA) equipped with a special adapter for fluorescence polarization measurements (Aminco-J4-9501). Complexes were labeled with diphenylhexatriene (DPH) and fluorescence polarization of the probe in the complexes with DPPC was measured as a function of temperature between 30 and 60°C.

Infrared Spectroscopy Measurements. Attenuated total reflection infrared spectroscopy (ATR-IR) was applied to determination of the secondary structure of native and lipid-bound apoE3 and the relative orientation of apolipoprotein helical segments and phospholipid acyl chains [20, 21]. A 70-µl sample of a solution containing 20 µg apoE3 (as native protein or present in the complexes) in 1 mM Tris-HCl buffer, pH 7.6, was spread on a germanium crystal plate. Deuteration of the sample was performed by flushing N_2 saturated with D_2O in a sealed universal Perkin-Elmer sample holder (Perkin-Elmer, USA) at room temperature for three hours, in order to avoid overlapping of the absorption bands of random and α-helical structures [21]. Spectra were recorded on a Perkin-Elmer 1720X infrared spectrophotometer (USA) using polarized incident light with a perpendicular (90°) and parallel (0°) orientation. The dichroic spectrum was obtained by subtracting the spectrum recorded with polarized light at 0° from that at 90°. The angle between a normal to the germanium crystal and the dipole was calculated from dichroic ratio $R = A_{90°}/A_{0°}$, representing the ratio of the absorbances with 90° and 0° polarizations. For each experiment, up to 15 scans were stored and averaged.

Circular Dichroism Measurements. Circular dichroism (CD) spectra of the native apolipoprotein and of the complexes were measured at 23°C in a Jasco 600 spectropolarimeter (Jasco, Japan) calibrated with 0.1% (w/v) d-10-camphorsulfonic acid [22]. Measurements were carried out at protein concentration of 0.1 mg/ml in 10 mM sodium phosphate buffer (pH 7.4). Nine spectra were collected and averaged for each sample. The percentage of α-helix was estimated from the ellipticity measurement at 222 nm (θ°_{222}) [23]:

$$\frac{\theta^{\circ}_{222} + 3000}{39000} \cdot 100\%,$$

and also by curve-fitting of the entire ellipticity curve between 184 and 260 nm according to the variable selection procedure developed by Johnson [24].

Denaturation Experiments. ApoE denaturation was followed by CD measurements after incubation of apolipoprotein solution and the complexes for 48 h at 4°C in 10 mM sodium phosphate buffer, pH 7.4, in the presence of guanidine hydrochloride (GdnHCl) at increasing concentrations. The molar ellipticity at 222 nm (θ_{222}) was calculated from the relationship:

$$\theta_{222} = \mathrm{MRW} \cdot \theta^{\circ}_{222}/10 \cdot l \cdot c,$$

where θ°_{222} is the measured ellipticity at 222 nm in degrees, l is the cuvette pathlength (0.1 cm), and c is the protein concentration in g/ml. The mean residue weight (MRW) for apoE3 is 114.4. The free energy of unfolding of apoE3, both in native and lipid-associated forms, was calculated from the changes in molar ellipticity at 222 nm, which were measured at increasing concentrations of GdnHCl. The calculations were carried out according to Sparks et al. [25]. The standard free energy of denaturation ΔG°_{D} is related to the free energy of denaturation ΔG_D and to GdnHCl mean ionic activity a by the equation:

$$G^{\circ}_{D} = \Delta G_D + \Delta n \cdot RT \ln(1 + ka),$$

where R is the gas constant, T the absolute temperature, k the average association constant of GdnHCl and protein

($0.6\ M^{-1}$), and Δn the difference in the moles of GdnHCl bound by the protein in native and denatured states. ΔG_D is related to molar ellipticities by the relation:

$$\Delta G_D = -RT\ \ln K_D = -RT\ \ln((\theta_N + \theta)/(\theta - \theta_D)),$$

where θ is the observed molar ellipticity at a given activity of GdnHCl and θ_N and θ_D are the corresponding values in native and fully denatured forms of the protein. The ΔG_D° and Δn values were obtained from linear regression of the denaturation curve ΔG_D versus a in the transition region.

LCAT Purification. LCAT was partially purified from the $d = 1.21$-$1.25\ g/cm^3$ fraction of normal human plasma by chromatography on Affi-gel Blue (LKB, Sweden) and DEAE-Sephadex (Pharmacia) [26]. A final purification factor of 5100 was obtained for the enzyme. The remaining impurities, detected by SDS-PAGE in a 10-25% gradient gel [27] and immunoblotting, consisted mainly of albumin. The enzyme was dialyzed against 10 mM Tris-HCl buffer (pH 7.6) containing 5 mM EDTA and stored at −70°C. Total protein was determined by the Bradford protein assay [28] with albumin as the standard. Scanning of the gels after Coomassie brilliant blue staining yielded an estimate of LCAT protein concentration of 52 μg/ml.

Substrate Properties of Complexes in the LCAT Reaction. LCAT activity in the presence of apoE3–PLPC–Chol complexes was determined by measuring the amount of cholesteryl esters by high performance liquid chromatography (HPLC) [29]. We used PLPC-complexes because of the lower detection limit in HPLC in comparison with DPPC-complexes. The assay mixture consisted of complexes at concentrations between 2 and 20 μM cholesterol to measure the initial velocity v_0 as a function of cholesterol concentration, 6 mM β-mercaptoethanol and 90 μM fatty acid-free bovine serum albumin (BSA) (Sigma). After 20 min preincubation at 37°C, the reaction was initiated by adding 5 μl of semi-purified LCAT to 0.2 ml of reaction mixture. The reaction was followed at 37°C up to 24 h and was stopped by addition of hexane–isopropanol (3:2 v/v) with cholesteryl heptadecanoate (Sigma) as internal standard. The initial velocities were determined from the linear portion of the curves corresponding to accumulation of cholesteryl ester up to 15%. The apparent kinetic parameters: V_{max}, K_m, and V_{max}/K_m were obtained by linear regression analysis of the data in the double reciprocal transform.

Conversion of Discoidal into Spherical Particles. When LDL are used as an external source of cholesterol, the LCAT reaction can be conducted to completion for 24 h, yielding spherical HDL-like particles as described by Vanloo et al. for the apoA-I–DPPC–Chol complexes [30]. Following these conditions, the incubation mixture contained 1 mg of the discoidal complexes (expressed as apolipoprotein), 1 mg LDL (expressed as apoB), 40 mg BSA, 10 mM β-mercaptoethanol, and 21 μg of semi-purified LCAT in a total volume of 1 ml. The samples were incubated under N_2 for 24 h at 37°C. The incubation products were isolated by density gradient ultracentrifugation in sucrose/NaCl gradient at densities between 1.02 and $1.20\ g/cm^3$ [31]. The reaction mixture was centrifuged for 66 h in Ti SW 41.0 rotor at 38,000 rpm in Beckman L7-65 ultracentrifuge (USA). The tubes were eluted with an autodensitoflow system and 0.5 ml fractions were collected. The optical density was measured at 280 nm in the flow-through cell of an SP6-400 Pye Unicam ultraviolet spectrophotometer (Pye Unicam Ltd, UK). The density of the fractions was determined by pycnometry. The protein was calculated from phenylalanine content measured by HPLC on C18 reversed-phase column after protein hydrolysis [22]. The purity of the fractions was checked by measuring apoB content by sandwich ELISA assay [32]. The spherical particles were characterized in the same way as described for discoidal complexes using EM, ATR-IR, and fluorescence polarization of DPH.

Cellular Cholesterol Efflux. J774 murine macrophages were grown in RPMI-1640 (Gibco Europe, Belgium) with addition of 10% heat inactivated fetal calf serum (FCS, Gibco Europe, Belgium) in a 5% CO_2 atmosphere. Cells were inoculated in 35 mm dishes at a density of $2 \cdot 10^6$ per dish, grown for 18 h in 2 ml RPMI with 10% FCS, and used as confluent monolayers. The cells were washed twice with RPMI and incubated with acetylated LDL at a concentration of 100 μg apoB/ml for 24 h in RPMI medium with 10% lipoprotein-deficient serum (LPDS). Cell monolayers were washed with RPMI and stored for 24 h in RPMI with 10% LPDS. The cholesteryl ester-loaded cells were incubated in 2 ml RPMI supplemented with 1 g/liter BSA. The discoidal apoE3–DPPC complexes were added to the medium at apolipoprotein concentrations varying between 0 and 100 μg/ml and the cells were incubated for 24 h. The experiments were carried out in the absence and in the presence of LCAT. In the latter case, 5 to 50 μl of semi-purified enzyme (52 μg/ml), dialyzed against 10 mM Tris-HCl buffer, pH 8.6, with 0.15 M NaCl, 0.1 mM dithiothreitol (DTT), and 100 μg complexes as apolipoprotein were added to the medium. After incubation, lipid extracts were prepared by addition of 5 ml hexane–isopropanol (3:2 v/v) [33] to 1 ml of the medium; 50 μl of chloroform solution of cholesteryl heptadecanoate and β-sitosterol at concentration of 0.5 mg/ml were added as internal standards for HPLC quantification of cholesteryl esters and cholesterol, respectively [34]. After vortex-mixing for 3 min and centrifugation at 3000 rpm for 15 min, the organic phase supernatant was dried and the precipitate was dissolved in 1 ml chloroform and washed three times. The dry residue was

TABLE 1. Distances between Charged Residues Forming Salt Bridges in Pairs of Helixes Linked by β-Strand in the C-Terminal Domain of ApoE3

1st helix	β-Strand	2nd helix	Ionic pair	Distance, Å	Angle, deg
206-221	222-226	227-242	R^{206}-E^{238}	4.0	24
			R^{206}-E^{231}	7.6	
			R^{213}-E^{231}	8.5	
			R^{213}-D^{227}	5.9	
			R^{217}-E^{231}	5.6	
			R^{217}-D^{227}	1.9	
227-243	244-247	248-264	D^{230}-K^{262}	3.2	15
248-264	265-269	270-286	–	–	90

TABLE 2. Composition and Size of DPPC and DPPC–Chol Complexes with ApoE3 before and after Incubation with LDL and LCAT

Original mixture	Incubated with	Phospholipid/Chol/ protein weight ratio in complex isolated	Phospholipid/Chol/ protein molar ratio in complex isolated	Complex diameter by GGE,[a] Å	Complex diameter by EM,[b] Å
ApoE3–DPPC	–	3.3:0:1	152:0:1	116 ± 2	138 ± 19
ApoE3–DPPC–Chol	–	3.4:0.17:1	158:15:1	116 ± 2	148 ± 19
ApoE3–DPPC–Chol	LDL + LCAT	2.8:0.6:1	129:52:1	–[c]	117 ± 19

[a]Obtained from gradient gel electrophoresis in non-denaturing gels by reference to standard proteins. The reproducibility of the values are within ±2 Å.
[b]Measured from electron micrographs of negatively stained samples. Means ± SD of the diameters are given for n = 175.
[c]An accurate determination of the diameter of the spheres by GGE was not possible.

finally dissolved in 50 μl chloroform–acetonitrile–isopropanol (1:1:1 v/v), of which 20 μl was injected into the HPLC system.

RESULTS

Computer Modeling of Helical Repeats of ApoE3. Since the helices in the C-terminal domain of apoE3 are mainly responsible for the lipid-binding properties of apoE [35, 36], we carried out an energy minimization procedure on the pairs of helices within sequences 206-242, 227-264, and 248-286, as these had been identified by internal homology search as the most probable helical repeats. The stereo alphabet procedure enabled calculation of the conformation of the 4-5-residue segment separating the helices (Fig. 1). A systematic analysis of the angles φ and ψ of these segments, followed by the simplex minimization procedure permitted calculation of the angle between the axes of the adjacent helices within sequences 206-242 (24°) and 227-264 (15°), i.e., these helices are almost parallel to each other. The helices spanning residues 248-286 are perpendicular since this angle is 90°. The residues able to form salt bridges between contiguous helices in the C-terminal domain of apoE3 within a distance of 10 Å are listed in Table 1. The residues within the sequence 206-242 seem to form the most stable pair of helices as six different ionic pairs between positive and negative residues could exist within this sequence. The three positively charged arginine residues 206, 213, and 217 can each interact with two negative glutamic or aspartic acid residues. Only in the last pair of helices no salt bridges are likely to exist since the distances between the charged residues of these two contiguous helices are more than 10 Å.

Structural and Substrate Properties of Discoidal Complexes. The discoidal complexes were isolated on a Superose 6HR column. The complex composition together with the size of the complexes is summarized in Table 2. Electron microscopic (EM) examination of the complexes revealed the typical pattern of rouleaux, characteristic of stacked discs. The size of the complexes assessed from EM data was about 25 Å larger than that obtained from gradient gel electrophoresis (GGE) [37]. The transition temperatures of DPPC reported by DPH fluorescence polarization (Fig. 2) were higher for apoE3–DPPC and apoE3–DPPC–Chol complexes (41.9 and 43.4°C, respectively) compared to the values for pure DPPC liposomes (41.2°C, data not shown) and DPPC–Chol liposomes (42.2°C). The Trp emission wavelength maximum was shifted from 343 nm for apoE3 in solution to 337 nm for apoE3–DPPC complexes (Table 3).

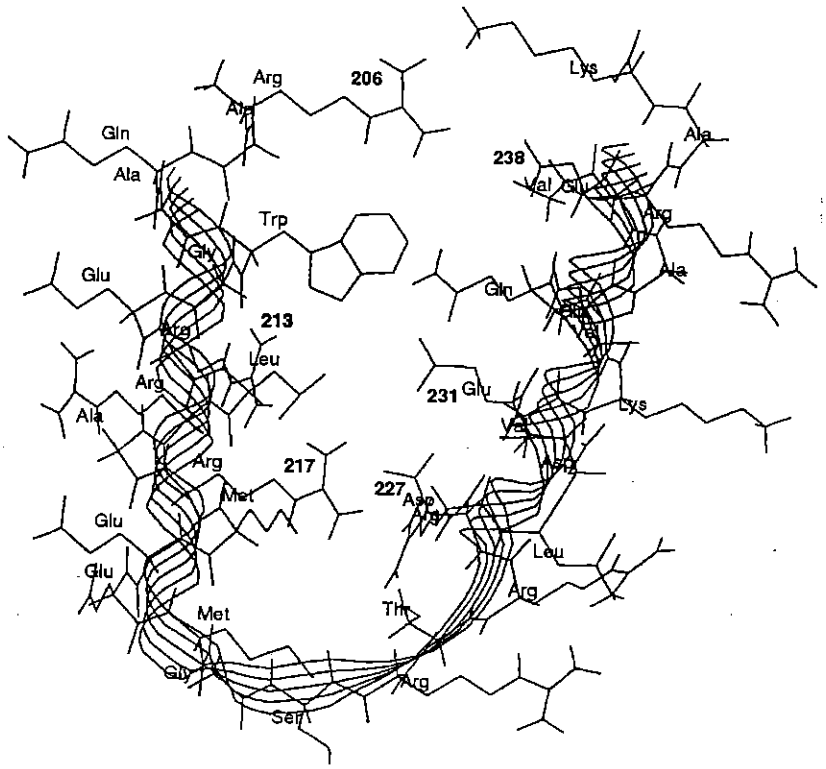

a

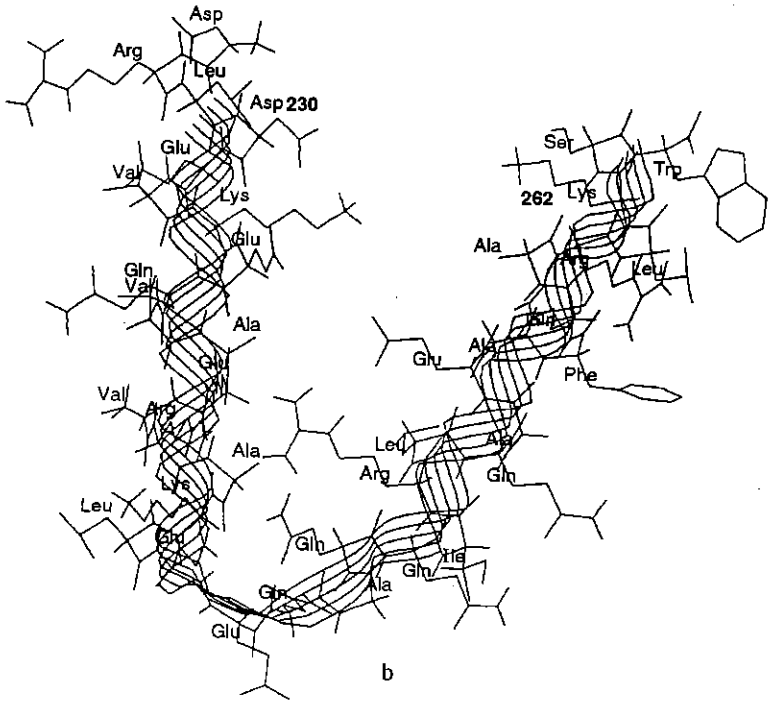

b

Fig. 1 (a and b).

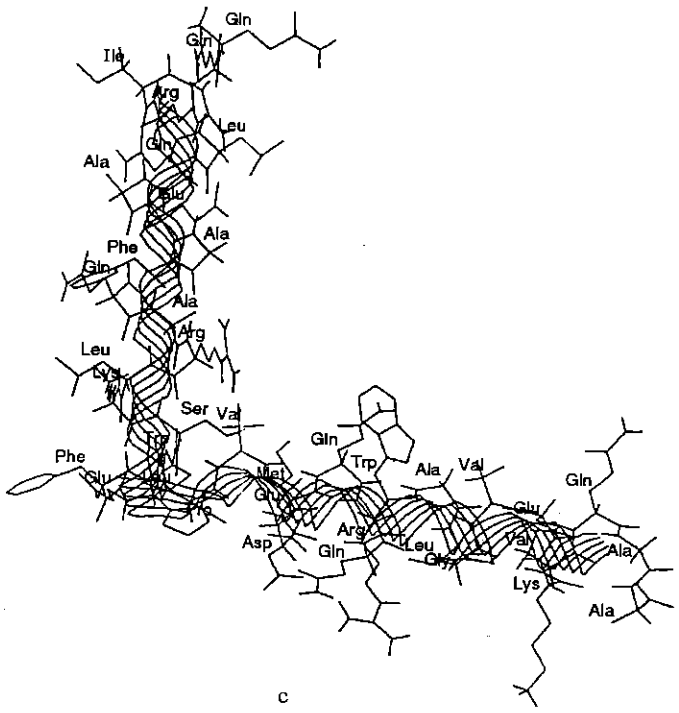

Fig. 1. Computer modeling by energy minimization of the pairs of helices separated by an extended β-strand in the C-terminal domain of apoE3: a) α-helix 206-221, β-strand 222-226, α-helix 227-242; b) α-helix 227-243, β-strand 244-247, α-helix 248-264; c) α-helix 248-264, β-strand 265-269, α-helix 270-286.

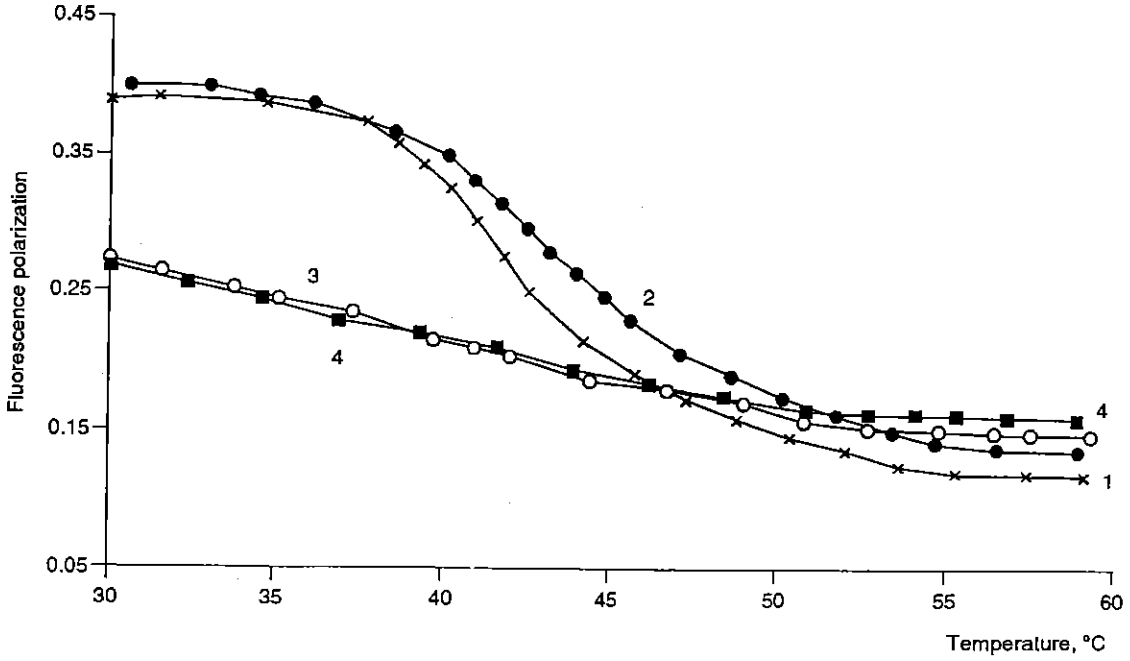

Fig. 2. DPH fluorescence polarization as a function of temperature: 1) DPPC–cholesterol liposome; 2) apoE3–DPPC–Chol complex; 3) apo E3–DPPC–Chol complex after incubation with LDL and LCAT; 4) HDL_3.

As followed from CD and infrared measurements, phospholipid binding increased the α-helical content in apoE by about 10% (Table 3). The calculated dichroic ratio R indicates that the hydrocarbon phospholipid chains are tilted at an angle of 20° and 22° from the normal to the germanium surface for the apoE3–DPPC

TABLE 3. Maximum Trp Emission Wavelength and α-Helix Content Determined by CD and IR Measurements in Native ApoE3 and the Apolipoprotein–DPPC Complexes[a]

Sample	Trp emission wavelength maximum, nm	α-Helix content, %		
		A	B	C
ApoE3	343	47	46	36
ApoE3–DPPC	337	59	59	44

[a] A, calculated according to Morrisett et al. [23]; B, calculated according to Johnson et al. [24]; C, calculated from ATR-IR data.

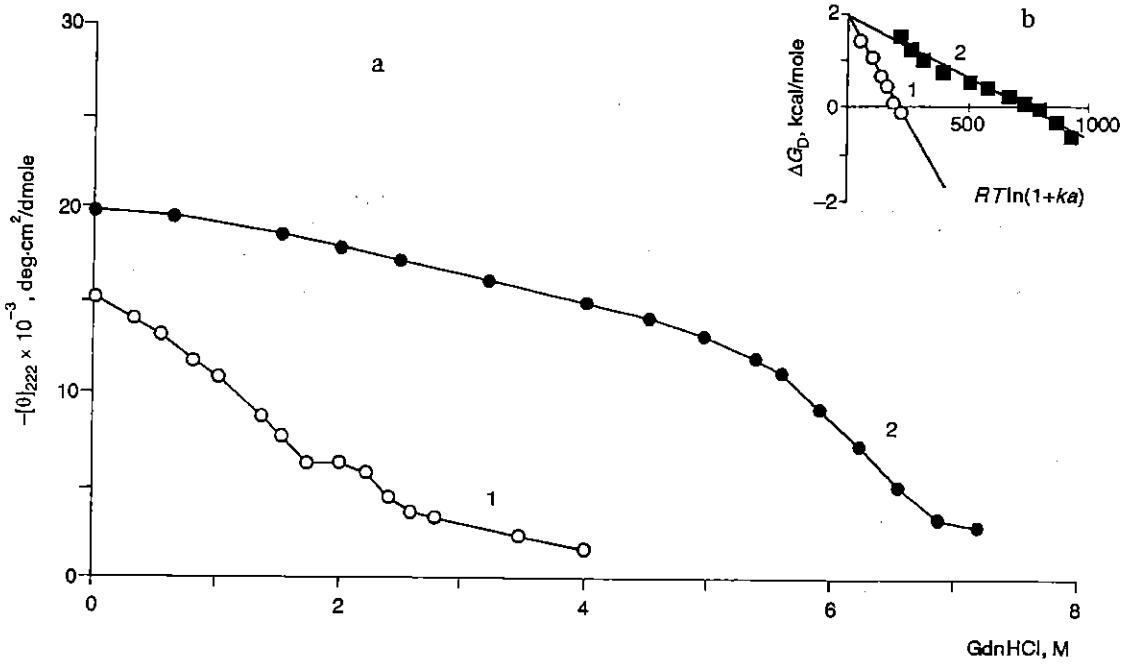

Fig. 3. a) GdnHCl-induced denaturation of native apoE3 (*1*) and apoE3–DPPC complexes (2) monitored by circular dichroism; θ_{222} is the molar ellipticity at 222 nm; b) linear transform of the data on apoE denaturation in solution (*1*) and within the complex (2). The standard free energy in water ΔG_D° and the number of moles of denaturant bound by the protein molecule Δn are calculated as the *y*-intercept and the slope of the regression lines, respectively (*a* is GdnHCl mean ionic activity).

and apoE3–DPPC–Chol complexes, respectively. The dichroic ratios of the α-helical component measured for the complexes apoE3–DPPC and apoE3–DPPC–Chol correspond to angles between the long axis of the α-helix and a normal to the germanium plate 30° and 32°, respectively. We can therefore assume that the helixes of apoE3 and the phospholipid acyl chains in the complexes are oriented in a parallel fashion.

Circular dichroism data on GdnHCl-induced denaturation of apoE3 in solution and within the apoE3–DPPC complexes are presented in Fig. 3. As the denaturant concentration was increased, the mean residue ellipticity at 222 nm θ_{222} became less negative, indicating a loss of secondary structure. The biphasic nature of the apoE3 denaturation curve suggests that there are at least two independently folded protein domains with different resistance to GdnHCl denaturation: the first transition midpoint at 1.2 M GdnHCl belongs to the C-terminal domain while the second transition at 2.4 M—to the N-terminal domain. The molar ellipticity values at 222 nm for the apoE3–DPPC complexes are higher than that for native apoE3 and show a monophasic curve that agrees with increased α-helical content of the complexes; the midpoint of denaturation of the apoE3–DPPC complexes is shifted towards higher GdnHCl concentrations (5.6 M) compared to the transition detected in native apoE3. Figure 3b includes data on the change of free energy of denaturation ΔG_D as a function of GdnHCl activity for the transition region of the denaturation curves of native apoE3 and the apoE3–DPPC complexes; for apoE3 in solution versus apoE3 within the complexes, the experimental data could not be fitted to a one-step

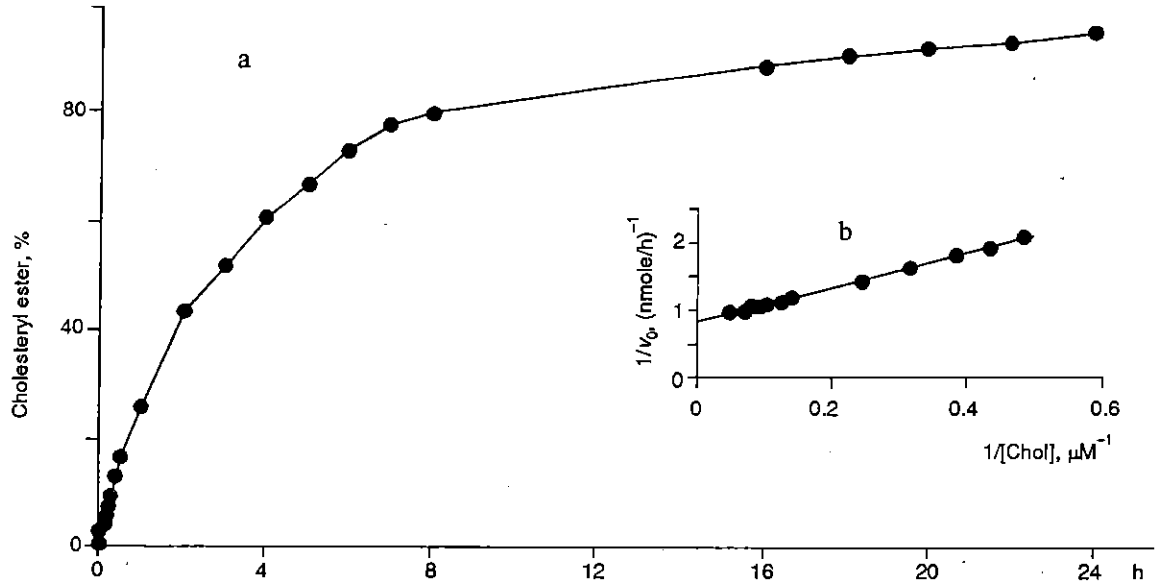

Fig. 4. a) Activation of the LCAT-catalyzed formation of cholesteryl ester in discoidal apoE3–PLPC–Chol complex; b) Lineweaver–Burk plot to calculate the kinetic parameter (v_0, initial reaction velocity).

model, probably due to the difference in stability of N- and C-terminal domains [38, 39]. As we did not measure the denaturation of these two domains separately, we could only calculate the denaturation parameters of the C-terminal domain of the native protein from the initial part of the denaturation curve. The number of moles of GdnHCl bound to apoE3 in the complex (2.6 moles GdnHCl per mole apoE) is less than for the native protein (9.1 moles GdnHCl per mole apoE) probably due to decreased accessibility of GdnHCl to the binding sites on the apolipoprotein within the complex [25].

The substrate properties of the complexes in the reaction with LCAT as well as their ability to accept cellular cholesterol served as functional characteristics of the complexes in our study. The kinetics of the LCAT reaction with the discoidal apoE3–PLPC–Chol complexes as substrates was followed between 0 and 24 h (Fig. 4a). Cholesterol esterification exceeded 90% after 24 h and the initial velocity values were calculated from the linear portion of the curve corresponding up to 15% esterification. A double reciprocal plot of the data is shown in Fig. 4b. The derived V_{max} = 1.2 nmoles cholesteryl esters/h and the K_m value, expressed as cholesterol concentration, is 2.6 μM. The substrate efficiency, expressed as V_{max}/K_m is 0.5 nmole/h per 1 μM. After 24 h incubation of Chol-loaded J774 macrophages with the discoidal apoE3–DPPC complexes, the amount of cholesterol released into the medium increased as a saturable function of the acceptor concentration (Fig. 5). Cholesterol efflux into the medium occurred only as free cholesterol as no cholesteryl esters were detected by HPLC. When the

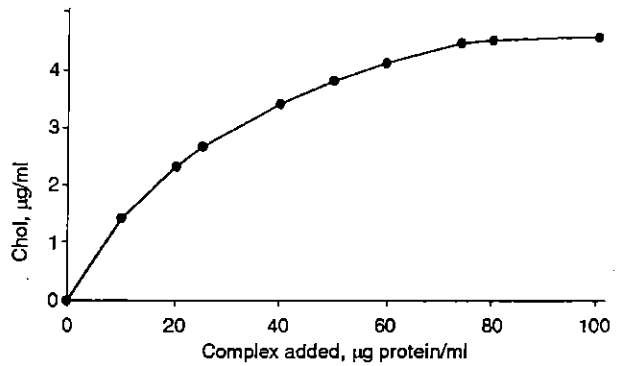

Fig. 5. Concentration dependence of cholesterol efflux from J774 macrophages into the medium after 24 h incubation of the cells with apoE3–DPPC complex.

cellular efflux was measured in the presence of LCAT (Fig. 6), cholesteryl palmitate was subsequently detected by HPLC, indicating that the enzyme was able to esterify the cholesterol-enriched apoE3–DPPC complexes. However, the total amount of cholesterol released into the medium did not increase in the presence of LCAT.

Characterization of Spherical Particles. The spherical particles obtained after incubation of discoidal apoE3–DPPC–Chol complexes with LDL and LCAT for 24 h were isolated by ultracentrifugation (Fig. 7). The apoB contamination of the apoE3–DPPC–Chol complexes is less than 5%. After incubation with LDL and LCAT, the phospholipid content decreased and the cholesterol content increased in the complex (Table 2) due to exchange

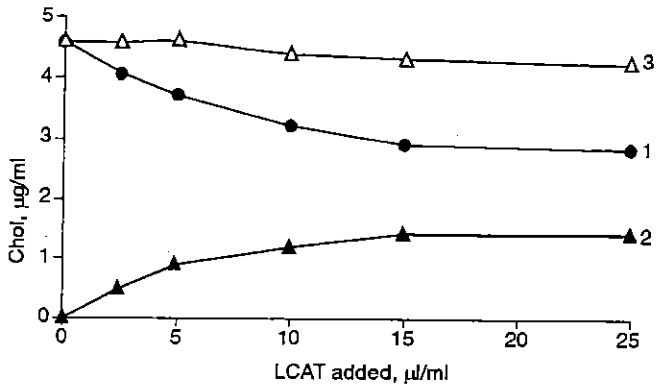

Fig. 6. Influence of LCAT on accumulation of cholesterol (1), cholesteryl esters (2), and total cholesterol (3) in the medium after incubation of J774 macrophages with apoE3–DPPC complexes.

with LDL [40]; 62% of the total cholesterol appears as cholesteryl esters. According to EM data, the transformation of the discoidal complexes into spherical particles resulted in a decrease in particle dimension (Fig. 7, Table 2). The percentage of α-helix did not change significantly after 24 h incubation with LDL and LCAT, but preferential orientation of the phospholipid acyl chains relative to a germanium plate disappeared as measured by ATR-IR. The parallel orientation of the long axis of the apolipoprotein helical segments with the phospholipid acyl chains disappeared almost completely in the spherical particles compared to the original discoidal complexes. Fluorescence polarization experiments carried out on the spherical particles (Fig. 2) showed a significant decrease in the amplitude of the DPPC transition in comparison with the transition observed for the discoidal complexes. The temperature response of the polarization ratio for the complexes after incubation with LDL and LCAT became close to that of an HDL_3 fraction, suggesting the formation of a cholesteryl ester core and the disappearance of the phospholipid bilayer in the converted particles.

DISCUSSION

In this study the lipid-binding and LCAT-activating properties of apoE3 were studied in order to define the mechanisms of association with lipid phase and to compare results with those previously reported for apoA-I [30, 37]. According to the current model of the structure of the discoidal complexes of apolipoprotein with phospholipid [37, 41], the lipid-binding domains of apoA-I and apoE3 consist of amphipathic helixes which are organized in pairs. The helixes are anti-parallel to each other inside one pair, as they are separated by β-strand which reverses the orientation of the second helix of the pair. The hydrophobic faces of the helixes are oriented towards the lipids while their polar face is facing the aqueous phase. Ionic interactions and salt bridge formation can further stabilize these pairs of helixes [42]. Analogous to calculations for apoE3 in our study, an energy minimization procedure was carried out on pairs of helixes 102-140, 124-162, 146-184, and 168-206 of the carboxyl-terminal domain of apoA-I [15]. Almost parallel orientation of the long axes of two helixes in the pairs of both apoA-I and apoE3 was observed in most of the pairs, except for the pair 102-140 of apoA-I where the angle between helixes is 67° and the pair 248-286 of apoE3 where the angle is 90°. In all the pairs except those of the apoE the last one, 248-286, salt bridges are formed between charged residues of the contiguous helixes within a distance of 10 Å. The mode of packing of helical segments in the carboxyl-terminal domains of apoA-I and apoE3 seems to be similar.

The size of the apoA-I–DPPC–Chol complexes measured by Vanloo et al. [30] is smaller than that of the complexes with apoE3 due to the difference in number of helixes within the complexes: 12 helixes per complex correspond to two molecules of apoA-I within the complex, while the apoE3–phospholipid complexes consist of 16 helixes per complex [41]. The properties of these complexes are similar in terms of protein and lipid content and apolipoprotein secondary structure [30, 37]. The Trp residues, however, are in a more polar environment in the apoE3–phospholipid complexes versus the apoA-I-containing complexes as followed from a blue shift of the fluorescence spectrum maximum for apoA-I–DPPC complexes (332 nm) compared to that for the apoE3–DPPC complexes (337 nm). The values of the maxima are comparable with those found by Jonas et al. [43] for free apoA-I, free apoE, and apolipoprotein–POPC–Chol complexes. In apoE3 molecule, five of the seven Trp residues at position 20, 26, 34, 39, and 210 belong to either the N-terminal or intermediate domains and only the C-terminal Trp residues 264 and 276 are sensitive to lipid-binding [44]. In the apoA-I molecule, Trp residues at position 50, 72, and 108 belong to helical repeats, and only Trp 8 does not belong to the lipid-binding domain.

The observed biphasic nature of apoE denaturation in solution (Fig. 3) is an indicator of the existence of stable intermediate forms during apolipoprotein unfolding and confirms two domain structure of apoE in solution suggested earlier [38, 39]. These two domains could not be resolved in the apoE3–phospholipid complex during its denaturation. It can be suggested that after association of the C-terminal end of the apolipoprotein molecule with lipid, the globular N-terminal domain, which exists as a four helix-bundle in solution [6], can undergo a conformational change in which the longer 36-residue helixes can bend around the central Pro or Gly residues to yield two 18-residue segments which can orient themselves parallel to the phospholipid acyl chains [45] and cover

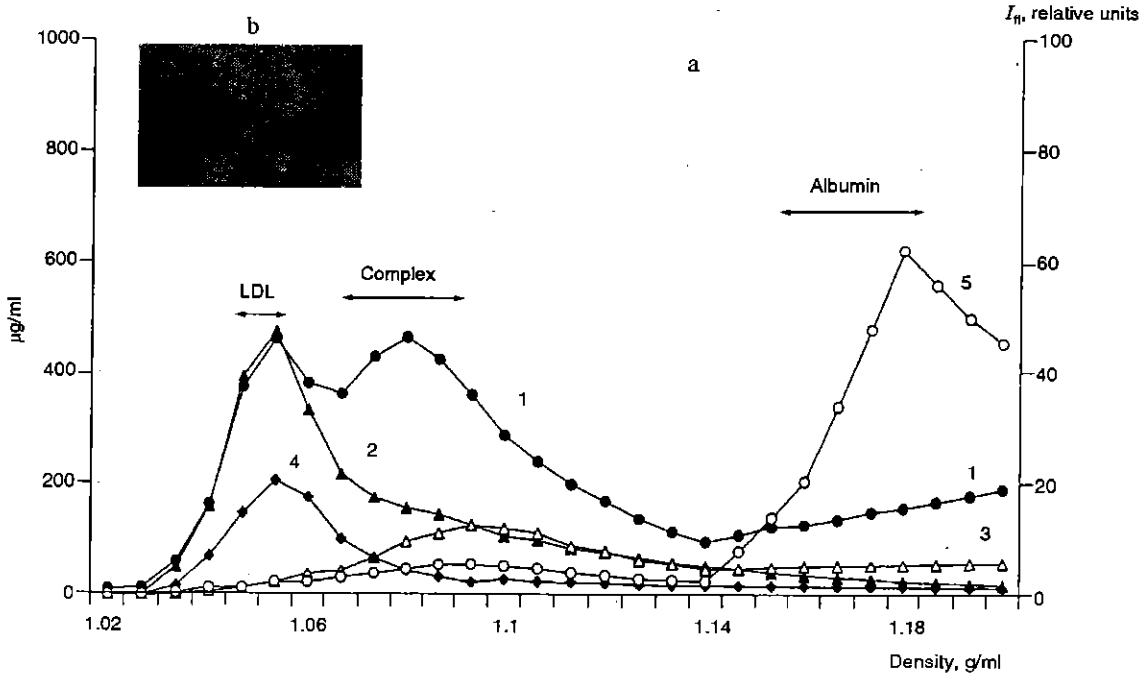

Fig. 7. a) Re-isolation of apoE3–DPPC–Chol complexes by density gradient ultracentrifugation after incubation of the complex with LDL, BSA, and LCAT for 24 h at 37°C: 1) DPPC; 2) Chol; 3) apoE3; 4) apoB. 5) Trp fluorescence. b) Electron micrograph of negatively stained re-isolated complexes.

the edge of the discoidal complexes. In comparison with apoE–POPC–Chol [43], apoE in the complex with DPPC (Fig. 3) possesses an increased stability, probably due to a destabilizing cholesterol action [46] originating from the competition between apolipoprotein and cholesterol molecules for the binding with phospholipid.

The existence of multiple sites in apoA-I molecule with different affinities to cholesterol and phospholipid has been suggested recently [47]. We suggest the same situation in the case of apoE and the differences in the functional properties of the complexes with apoA-I and apoE could therefore originate from the different intradomain organization of these apolipoprotein molecules. As a result, the local concentration of cholesterol molecules and/or their orientation and mobility in close vicinity to Chol-binding sites could differ and result in the 7-fold increase of V_{max} for the LCAT reaction with apoA-I–PLPC–Chol complexes (9.5 nmoles cholesteryl esters/h, data not shown) compared to that with apoE-containing complex (Fig. 4).

As LCAT-catalyzed cholesterol esterification proceeded to completion in 24 h, the disc-to-sphere conversion was observed with the disappearance of preferential orientation of helical segments of the protein relative to phospholipid acyl chains, as observed with apoA-I–phospholipid complexes [30]; the amplitude of the phospholipid phase transition decreased, probably, due to stabilizing action of cholesteryl ester observed also for the spherical particles with apoA-I [48]. The cholesteryl ester content was 62% in the apoE3–DPPC–Chol complexes compared to 86% in the complexes with apoA-I [30], accounting for the formation of the spherical core. The higher percentage of cholesteryl esters found for apoA-I is in agreement with the better LCAT activating properties of apoA-I. Our results for apoE3 agree well with 67% cholesterol esterification found by Gong et al. [49] for apoE–POPC–Chol complexes. The phospholipid/apoE ratio measured in the spherical complexes (2.8:1 w/w) is approximately three times higher than that of the apoE-containing HDL particles in plasma [50]. This means that if such a phospholipid-enriched product is formed *in vivo*, its composition has to change by transfer or hydrolysis of phospholipids in order to reach a composition similar to that of plasma apoE-containing HDL.

The cholesterol efflux from cholesterol-loaded J774 macrophages towards discoidal apoE3–DPPC complexes (Figs. 5 and 6) is about 62% of that in the presence of apoA-I–DPPC complexes [51]. The total amount of cholesterol released from the cells is, however, not affected by the presence of LCAT and by the formation of cholesteryl esters within discoidal particles, i.e., these two

processes might belong to two different independent metabolic compartments. Like the influence on LCAT activity, lipid-bound apoA-I, apoA-IV, and apoE seem to act as the most efficient promoters of cholesterol efflux compared to apoA-II-containing HDL subfractions [52]. When discoidal particles acquire cholesterol, they transform gradually into mature HDL by LCAT. The esterified cholesterol can be transferred to VLDL and LDL through the action of cholesteryl ester transfer protein (CETP) or catabolized in the liver together with HDL [53]. A comparison of the substrate properties of the discoidal complexes with apoE and apoA-I in LCAT reaction suggests more significant relative contribution of the precursor system with apoA-I compared with apoE towards the synthesis of mature plasma HDL; however, in the case of the absence or deficiency of apoA-I, apoE could play a major role in this process. It can be suggested that despite a general similarity of structural organization of apolipoproteins E and A-I in lipid-bound form, the highest functional activity of apoA-I-containing particles could originate from the quantitative differences in the interaction of α-helical regions of apoE and apoA-I molecules with Chol–phospholipid phase. In particular, the concentration of cholesterol molecules and/or their orientation and dynamics could differ in the phospholipid region close to the apolipoprotein molecule ("boundary lipid"). Experiments are now in progress to visualize the structural/compositional peculiarities of the protein–lipid interface in apoE-, apoA-II-, and apoA-I-containing complexes.

During this study, M. De Pauw was a recipient of a fellowship of IWONL (Instituut tot aanmoediging van het Wetenschappelijk Onderzoek in Nijverheid en Landbouw) and A. D. Dergunov was the recipient of a European Society of Cardiology Research Training Fellowship. We are grateful to G. Michiels, C. Tilleman, J. Taveirne, and H. Caster for their excellent technical assistance and to C. Labeur for critical reading of the manuscript.

LITERATURE CITED

1. Mahley, R. W., and Innerarity, T. L. (1983) *Biochim. Biophys. Acta*, **737**, 197-222.
2. Dergunov, A. D., and Rosseneu, M. (1994) *Biol. Chem. Hoppe-Seyler*, **375**, 485-495.
3. Rall, S. C., Jr., Weisgraber, K. H., and Mahley, R. W. (1982) *J. Biol. Chem.*, **257**, 4171-4178.
4. McLean, J. W., Elshourbagy, N. A., Chang, D. J., Mahley, R. W., and Taylor, J. M. (1984) *J. Biol. Chem.*, **259**, 6498-6504.
5. Zannis, V. I., McPherson, J., Goldberger, G., Karathanasis, S. K., and Breslow, J. L. (1984) *J. Biol. Chem.*, **259**, 5495-5499.
6. Wilson, C., Wardell, M. R., Weisgraber, K. H., Mahley, R. W., and Agard, D. A. (1991) *Science*, **252**, 1817-1822.
7. Eisenberg, S. (1984) *J. Lipid Res.*, **25**, 1017-1058.
8. Tall, A. R., Small, D. M., Deckelbaum, R. J., and Shipley, G. G. (1977) *J. Biol. Chem.*, **252**, 4701-4711.
9. Jonas, A. (1984) *Exp. Lung Res.*, **6**, 255-270.
10. Chen, C. H., and Albers, J. J. (1985) *Biochim. Biophys. Acta*, **836**, 279-285.
11. Ross, R. (1986) *N. Engl. J. Med.*, **314**, 488-495.
12. Brown, M. S., and Goldstein, J. L. (1983) *Annu. Rev. Biochem.*, **52**, 223-261.
13. Hara, H., and Yokoyama, S. (1991) *J. Biol. Chem.*, **266**, 3080-3086.
14. Rosseneu, M., De Loof, H., De Meutter, J., Ruysschaert, J. M., and Brasseur, R. (1990) in *Molecular Description of Biological Membrane Components by Computer Aided Conformational Analysis*, Vol. II (Brasseur, R., ed.) CRC Press, Boca Raton, pp. 173-190.
15. Vanloo, B., Rosseneu, M., De Pauw, M., Lins, L., Brasseur, R., and Ruysschaert, J. M. (1993) in *Drugs Affecting Lipid Metabolism* (Catapano, A., Gotto, A. M., Smith, L., and Paoletti, R., eds.) Kluwer Acad., Dordrecht, pp. 49-56.
16. Brasseur, R. (1991) *J. Biol. Chem.*, **266**, 16120-16127.
17. Havekes, L. M., de Knijff, P., Beisiegel, U., Havinga, J., Smit, M., and Klasen, E. (1987) *J. Lipid Res.*, **28**, 455-463.
18. Matz, C. E., and Jonas, A. (1982) *J. Biol. Chem.*, **257**, 4535-4540.
19. Bury, J., Vercaemst, R., Rosseneu, M., and Belpaire, F. (1986) *Clin. Chem.*, **32**, 265-270.
20. Cabiaux, V., Brasseur, R., Wattiez, R., Falmagne, P., Goormaghtigh, E., and Ruysschaert, J. M. (1989) *J. Biol. Chem.*, **264**, 4928-4939.
21. Goormaghtigh, E., Brasseur, R., Haurt, P., and Ruysschaert, J. M. (1987) *Biochemistry*, **26**, 1789-1794.
22. Brasseur, R., De Meutter, J., Vanloo, B., Goormaghtigh, E., Ruysschaert, J. M., and Rosseneu, M. (1990) *Biochim. Biophys. Acta*, **1043**, 245-252.
23. Morrisett, J. D., David, J. S. K., Pownall, H. J., and Gotto, A. M., Jr. (1973) *Biochemistry*, **12**, 1290-1299.
24. Johnson, W. C., Jr. (1990) *Proteins*, **7**, 205-214.
25. Sparks, D. L., Lund-Katz, S., and Phillips, M. C. (1992) *J. Biol. Chem.*, **267**, 25839-25847.
26. Jonas, A. (1986) *J. Lipid Res.*, **27**, 689-698.
27. Laemmli, U. K. (1970) *Nature*, **227**, 680-685.
28. Bradford, M. M. (1976) *Anal. Biochem.*, **72**, 248-254.
29. Vercaemst, R., Rosseneu, M., De Craene, I., De Backer, G., and Kornitzer, M. (1989) *Atherosclerosis*, **78**, 245-250.
30. Vanloo, B., Taveirne, J., Baert, J., Lorent, G., Lins, L., Ruysschaert, J. M., and Rosseneu, M. (1992) *Biochim. Biophys. Acta*, **1128**, 258-266.
31. Rosseneu, M., Schmitz, G., Taveirne, M. J., and Assmann, G. (1984) *J. Lipid Res.*, **25**, 111-120.
32. Bury, J., and Rosseneu, M. (1988) *Rev. Immunoassay Techn.*, **1**, 1-25.
33. Mahlberg, F. H., Glick, J. M., Jerome, W. G., and Rothblat, G. H. (1990) *Biochim. Biophys. Acta*, **1045**, 291-298.
34. Vercaemst, R., Union, A., and Rosseneu, M. (1989) *J. Chromatogr.*, **494**, 43-52.
35. Aggerbeck, L. P., Wetterau, J. R., Weisgraber, K. H., Wu, C. C., and Lindgren, F. T. (1988) *J. Biol. Chem.*, **263**, 6249-6258.
36. Atkinson, D., and Small, D. M. (1986) *Annu. Rev. Biophys. Biophys. Chem.*, **15**, 403-456.
37. Vanloo, B., Morrisson, J., Fidge, N., Lorent, G., Lins, L., Brasseur, R., Ruysschaert, J. M., Baert, J., and Rosseneu, M. (1991) *J. Lipid Res.*, **32**, 1253-1264.
38. Wetterau, J. R., Aggerbeck, L. P., Rall, S. C., and Weisgraber, K. H. (1988) *J. Biol. Chem.*, **263**, 6240-6248.
39. Dergunov, A. D., Shuvaev, V. V., and Yanushevskaja, E. V. (1992) *Biol. Chem. Hoppe-Seyler*, **373**, 323-331.
40. Jonas, A., Kezdy, K. E., Williams, M. I., and Rye, K. A. (1988) *J. Lipid Res.*, **29**, 1349-1357.
41. Brasseur, R., Lins, L., Vanloo, B., Ruysschaert, J. M., and Rosseneu, M. (1992) *Proteins: Structure, Function, and Genetics*, **13**, 246-257.
42. Rosseneu, M., Vanloo, B., Lins, L., Corijn, J., Van Biervliet, J. P., Ruysschaert, J. M., and Brasseur, R. (1992) in *High Density Lipoproteins and Atherosclerosis*, Vol. III (Miller, N. E., and Tall, A. R., eds.) Elsevier, Amsterdam, pp. 105-114.
43. Jonas, A., Steinmetz, A., and Churgay, L. (1993) *J. Biol. Chem.*, **268**, 1596-1602.

44. Rosseneu, M., De Pauw, M., Vanloo, B., Dergunov, A., Weisgraber, K., and Brasseur, R. (1995) in *Atherosclerosis X* (Woodford, F. P., Davignon, J., and Sniderman, A., eds.) Elsevier, Amsterdam, pp. 651-655.
45. Wardell, M. R., Wilson, C., Agard, D. A., Mahley, R. W., and Weisgraber, K. H. (1993) in *Human Apolipoprotein Mutants, NATO ASI Series*, Vol. III (Sirtori, C. R., Franceschini, G., and Brewer, B.H., Jr., eds.) Springer-Verlag, Berlin, pp. 81-96.
46. Sparks, D. L., Davidson, W. S., Lund-Katz, S., and Phillips, M. C. (1993) *J. Biol. Chem.*, **268**, 23250-23257.
47. Meng, Q.-H., Bergeron, J., Sparks, D. L., and Marcel, Y. L. (1995) *J. Biol. Chem.*, **270**, 8588-8596.
48. Sparks, D. L., Davidson, W. S., Lund-Katz, S., and Phillips, M. C. (1995) *J. Biol. Chem.*, **270**, 26910-26917.
49. Gong, E. L., Nichols, A. V., Weisgraber, K. H., Forte, T. M., Shore, V. G., and Blanche, P. J. (1989) *Biochim. Biophys. Acta*, **1006**, 317-328.
50. Weisgraber, K. H., and Mahley, R. W. (1980) *J. Lipid Res.*, **21**, 316-325.
51. Rosseneu, M., Devreese, A. M., Vanloo, B., and Baert, J. (1993) in *Human Apolipoprotein Mutants, NATO ASI Series*, Vol. III (Sirtori, C. R., Fransceschini, G., and Brewer, B. H., Jr., eds.) Springer-Verlag, Berlin, pp. 21-30.
52. Barkia, A., Puchois, P., Ghalim, N., Torpier, G., Barbaras, R., Ailhaud, G., and Fruchart, J. C. (1991) *Atherosclerosis*, **87**, 135-146.
53. Tall, A. R. (1993) *J. Lipid Res.*, **34**, 1255-1273.